

Fluctuations in Repressor Control: Thermodynamic Constraints on Stochastic Focusing

Otto G. Berg,* Johan Paulsson,[†] and Måns Ehrenberg[†]

*Department of Molecular Evolution, Evolutionary Biology Centre, and [†]Department of Cell and Molecular Biology, Biomedical Center, Uppsala University, SE-75124 Uppsala, Sweden

ABSTRACT The influence of fluctuations in molecule numbers on genetic control circuits has received considerable attention. The consensus has been that such fluctuations will make regulation less precise. In contrast, it has more recently been shown that signal fluctuations can sharpen the response in a regulated process by the principle of stochastic focusing (SF) (Paulsson et al., 2000, *Proc. Natl. Acad. Sci. USA.* 97:7148–7153). In many cases, the larger the fluctuations are, the sharper is the response. Here we investigate how fluctuations in repressor or corepressor numbers can improve the control of gene expression. Because SF is found to be constrained by detailed balance, this requires that the control loops contain driven processes out of equilibrium. Some simple and realistic out-of-equilibrium steps that will break detailed balance and make room for SF in such systems are discussed. We conclude that when the active repressors are controlled by corepressor molecules that display large (“coherent”) number fluctuations or when corepressors can be irreversibly removed directly from promoter-bound repressors, the response in gene activity can become significantly sharper than without intrinsic noise. A simple experimental design to establish the possibility of SF for repressor control is suggested.

INTRODUCTION

Regulation of intracellular processes is inevitably subject to noise, partly because regulatory systems operate in randomly changing extra- or intracellular environments, but also because the reactions involve chemical species that are present in low copy numbers. It has been commonly assumed that the internal signal noise associated with low copy numbers must reduce precision of control by randomizing the response (Berg, 1978; Ko, 1992; Guptasarma, 1995; McAdams and Arkin, 1997, 1999; Arkin et al., 1998; Paulsson and Ehrenberg, 1998; Cook et al., 1998). A suitable parameter to quantify the sensitivity and quality of a molecular control mechanism is its amplification factor, measured as the percentage change in the response over the percentage change of the signal (see Savageau (1976) for an introduction).

In contrast to previous beliefs that noise impairs the sensitivity of control, it was recently shown (Paulsson et al., 2000) that internal noise in cellular control systems also can be exploited to increase, rather than decrease, sensitivity amplification by stochastic focusing (SF). It was demonstrated how random signal fluctuations can reduce random fluctuations in controlled processes, e.g., plasmid copy numbers (Paulsson and Ehrenberg, 2000). SF is based on the general principle that average reaction rates depend not only on average concentrations but also on the random variations in them (Renyi, 1953). SF may emerge in all

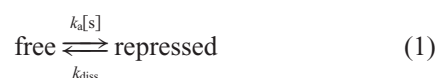
systems where reaction rates depend nonlinearly on randomly fluctuating concentrations.

Both of our previous analyses (Paulsson et al., 2000; Paulsson and Ehrenberg, 2000) treated a regulatory standard motif: hyperbolic inhibition arising from branching reactions. In the present analysis we extend the description of SF also to control mechanisms of the repressor-operator type. It is shown how SF is constrained by detailed balance and how its sensitivity-enhancing properties depend on “coherent” fluctuations and out-of-equilibrium binding reactions. “Coherent” in this context means fluctuations larger than the single-molecule deviations typical of Poisson or binomial distributions.

The mathematics of this paper is based on probability theory and mesoscopic kinetics, i.e., birth-and-death master equations. We first derive the appropriate mesoscopic equations for repressor-operator binding and show that fluctuations can significantly increase the sensitivity of control (SF), but only when detailed-balance constraints are violated. Then, the results are compared with the original concepts and models for SF (Paulsson et al., 2000; Paulsson and Ehrenberg, 2000). We also discuss a simple set of experiments, which can be based on, e.g., the *lac* repressor system and used to verify SF for repressor control of gene expression.

REPRESSOR-OPERATOR BINDING, FLUCTUATIONS, AND DETAILED BALANCE

Repressors are protein molecules that, on binding to a specific operator site on DNA, block the expression of an operon. For simple two-state reactions where the operator can be in a repressed or free state according to



Received for publication 6 July 2000 and in final form 6 September 2000.

Address reprint requests to Dr. Måns Ehrenberg, Department of Cell and Molecular Biology, Biomedical Center, Box 596, Uppsala University, SE-75124 Uppsala, Sweden. Tel.: 46-18-471-4213; Fax: 46-18-530396; E-mail: ehrenberg@xray.bmc.uu.se.

© 2000 by the Biophysical Society

0006-3495/00/12/2944/10 \$2.00

the probability that it is free, and that the gene(s) is consequently active, is given by the macroscopic binding relation

$$P_{\text{act}} = \frac{1}{1 + [s]/K} \quad (2)$$

where $K = k_{\text{diss}}/k_a$ and $[s]$ is the concentration of free repressor. At cell volume v , the concentration is determined by the number n of signal molecules as $[s] = n/v$. In macroscopic descriptions, a concentration is determined by the underlying rate constants, time, and initial conditions. However, at low copy numbers it is necessary to amend the macroscopic relation, Eq. 2, in two ways. First, the concentration of free repressor should be the calculated as the concentration conditional on the operator site being free (Berg and Blomberg, 1977). Second, the probabilistic nature of all chemical reactions and the consequent random fluctuations in molecule numbers must be accounted for (Paulsson et al., 2000). At this more realistic level of description, rate constants (transition probabilities per time unit) only determine the evolution of probability distributions, rather than the time behavior of concentrations.

To illustrate the principles involved we will first consider a simplified case where the activity of the controlled gene is determined directly by the total number of repressors in the system. Then we will expand the description to situations where the signal is instead the number of corepressors or inducers in the cell, which in turn determines the number of active (i.e., DNA-binding) repressors.

Consider a cell that contains one operator site and, with probability p_n , a total of n repressor molecules. If p_n^f and p_n^b denote the probabilities that there are n repressor molecules in the system and that the operator is free or bound, respectively, then their sum is the total probability that there are n repressors, i.e., $p_n = p_n^f + p_n^b$. The stationary distributions of free and bound repressors must be such that the overall rate of binding equals the overall rate of dissociation:

$$k_a' \sum_n n p_n^f = k_{\text{diss}} \sum_n p_n^b \quad (3)$$

Here we have introduced the association rate constant k_a' normalized by cell volume v and counted per molecule so that $k_a' = k_a/v$, where k_a is defined by Eq. 1. Introducing the dissociation constant K ($Kv = k_{\text{diss}}/k_a'$) as defined just below Eq. 2 above, it follows from Eq. 3 that the total probability, $P_{\text{act}} = \sum_n p_n^f$, that the operator is free satisfies the relation

$$\langle n \rangle_f P_{\text{act}} = Kv(1 - P_{\text{act}}) \quad (4a)$$

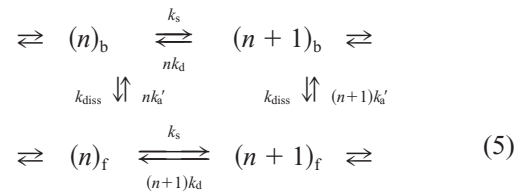
This can be rewritten as

$$P_{\text{act}} = \sum_n p_n^f = \frac{1}{1 + \langle n \rangle_f / Kv} \quad (4b)$$

Here $\langle n \rangle_f = \sum n p_n^f / \sum p_n^f$ is the conditional average number of repressor molecules in the system, given that the operator is

free. This result is very general because it only requires that the law of mass action holds, i.e., that the rate of binding of a free operator is proportional to the number of repressor molecules in the system, and that dissociation is a simple decay.

The impact of detailed balance on repressor-controlled gene expression will first be illustrated by a simple example. Assume that repressors are synthesized with constant rate, k_s , and degraded in proportion to the number of free molecules with first-order rate constant k_d . When there is one operator site that can bind only one repressor, the state of the system (cell) can be characterized with two parameters: n for the number of repressors present, and the operator site being bound or free. Denoting by $(n)_b$ and $(n)_f$ the states with n repressors in the system and with the operator bound and free, respectively, one of the loops of the complete mesoscopic reaction scheme will be



The detailed balance condition for chemical loops like the one in Scheme 5 is that the product of all rate constants in the clockwise direction should equal the product of all reverse rate constants. This is equivalent to the requirement that there is no net flux across any step at the stationary state (Eisenberg and Crothers, 1979; Berg, 1983). It is easy to see that Scheme 5 satisfies detailed balance, as do elementary schemes where active repressors are created from inactive precursors. In the latter case, if N is the total number of repressors and n is the number of active ones, the requirement is that the rate of activation is proportional to the number, $N - n$, of inactive precursors and the rate of deactivation is proportional to the number of free active repressors, n in state $(n)_f$ and $n - 1$ in state $(n)_b$. Then the horizontal synthesis (or activation) steps in Scheme 5 would have rates $(N - n)k_s$ for activation (rightward arrows) and $k_d n$ and $k_d(n - 1)$, respectively, for the deactivation. This ensures a balance against the binding steps of the loop where the rates by mass action are proportional to the number of free repressors.

When detailed balance is satisfied, the stationary distribution will always be such that there is no net flux across any of the reaction steps and each of the binding-dissociation steps will be balanced individually,

$$k_a' n p_n^f = k_{\text{diss}} p_n^b, \quad \text{for all } n > 0 \quad (6)$$

rather than just on average, as required by the more general Eq. 3. For Eq. 6 to hold, all other steps in the scheme must also be balanced.

The number of repressor molecules in a cell determines the gene activity. However, the cell can adjust the repressor numbers by changing the underlying rates, k_s and k_d , for synthesis (activation) and degradation (deactivation) of repressor molecules. Thus k_s and k_d serve as the control parameters with which the level of gene activity is set. The ratio k_s/k_d will be considered as the primary signal that determines the level of gene activity, i.e., the response. If the identification $[s] = \langle n \rangle / \nu$ is made, then Eq. 4b closely resembles the macroscopic relation, Eq. 2, except that it involves a conditional ($\langle n \rangle_f$) rather than a global ($\langle n \rangle$) average.

The consequence of detailed balance is that the relationships between individual states are totally independent of the rest of the scheme. In particular, the conditional average $\langle n \rangle_f$ in Eq. 4b can be calculated by considering only the free-operator states (the bottom row in Scheme 5). As a consequence, the activity and the response to change as given by Eq. 4b will be determined solely by whatever process regulates the free repressor numbers. When this is a linear process, as assumed in the two simple examples above, the conditional average $\langle n \rangle_f$ will always be linear in the primary signal parameter ($\langle n \rangle_f = k_s/k_d$ for Scheme 5). In fact, the probability distribution of the number of free repressors, given bound operator (p_n^b , upper row) and given free operator (p_n^f , lower row), in Scheme 5 will both be Poissonian, but the distribution (p_n) of the total number of repressors will not. In summary, when repressor fluctuations and binding reactions satisfy detailed balance, the repression curve, Eq. 4, will be hyperbolic, just like the macroscopic expectation, Eq. 2, and the intrinsic fluctuations cannot enhance sensitivity by SF. However, the fact that Scheme 5 and similar variants satisfy detailed balance depends on particular assumptions, which are atypical for many intracellular chemical reactions.

BREAKING DETAILED BALANCE

One critical assumption in Scheme 5 is that repressors can only be degraded when they are in the free, unbound state. Another is that repressors are synthesized and degraded as single molecules and not through bursts or some other process that would make fluctuations coherent.

One way of breaking detailed balance is therefore to allow degradation (deactivation) to take place also for a repressor molecule that is bound at the operator. This would introduce diagonal arrows with rates k_d from $(n+1)_b$ to $(n)_f$ for each $n \geq 0$ in Scheme 5. Because these arrows would be unidirectional, detailed balance can no longer hold. The probability distribution from the resulting scheme has been solved (see Appendix, Eq. A10), giving P_{act} from Eq. 4 as an integral involving all of the parameters (k'_a , k_{diss} , k_s , k_d). In Fig. 1 the expected activity, P_{act} , is plotted in a log-log scale versus the average number of repressors in the system, $\langle n \rangle = k_s/k_d$. The sensitivity amplification is defined (e.g.,

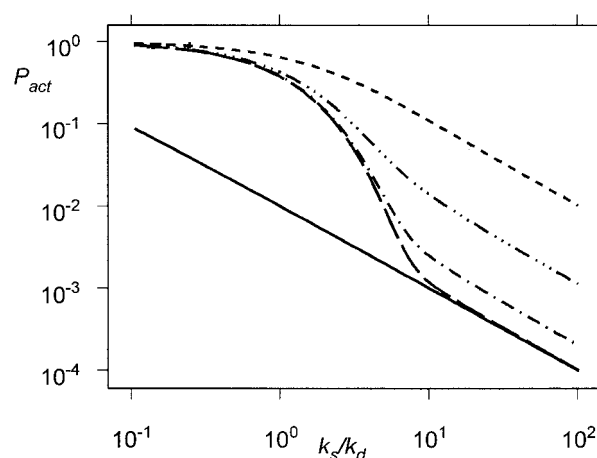


FIGURE 1 Gene activity as a function of $\langle n \rangle = k_s/k_d$ when $K\nu = 0.01$. —, Hyperbolic result from Scheme 5, where detailed balance holds. The other curves show the results when degradation can take place also for operator-bound repressor (Eq. A10): —, k'_a , $k_{diss} \gg k_d$; - · -, $k'_a/k_d = 100$; - · · · -, $k'_a/k_d = 10$; · · · · ·, $k'_a/k_d = 1$.

Savageau, 1976) as the relative change in response divided by the relative change in signal. This corresponds to the slope in a log-log plot of the signal-response curve (Fig. 1). Maximum sensitivity (i.e., maximum slope in the diagram) occurs in the limit $k_{diss}/k_d > 1$ (Fig. 1, dashed curve), where a small change in the primary signal can lead to a dramatic change in activity. In this limit, fluctuations in repressor numbers lead to a significantly increased sensitivity in control (SF) (Paulsson et al., 2000). For large values of $\langle n \rangle$, where $\langle n \rangle_f \approx \langle n \rangle$, all curves behave as expected from Eq. A3 in the Appendix. When $k'_a/k_d < 1$, Eq. A3 holds with $\langle n \rangle_f$ replaced by $\langle n \rangle$ throughout; i.e., in this limit, the result is like the macroscopic expectation, Eq. 2, with an effective dissociation constant $K' = (k_{diss} + k_d)/k'_a$ (Fig. 1, dotted curve).

Another interesting and biologically important situation where detailed balance cannot be satisfied is when repressors are synthesized in bursts (Berg, 1978; Paulsson et al., 2000). This can easily be seen from Eq. 6 since fulfillment of detailed balance would require that degradation occurs in bursts with the same distributions as the bursts of synthesis, which is virtually impossible. In this case we have no analytical solution, but numerical integration described in the Appendix confirms that stochastic focusing occurs when the inequality $k_{diss} > k_d$ is satisfied. This can be seen in Fig. 2, where the slopes in the log-log plots of the activity, P_{act} , versus average repressor numbers exceed those of the macroscopic expectation in some parameter regions. For each curve, the average burst size, β , is constant and the average repressor numbers are varied by changing the ratio k_s/k_d . The effects are largest for small K (strong binding) and large burst sizes (large fluctuations), as noted before for another system (Paulsson et al., 2000). The curves approach the macroscopic expectation with no SF when $k_{diss} \ll k_d$ (Fig.

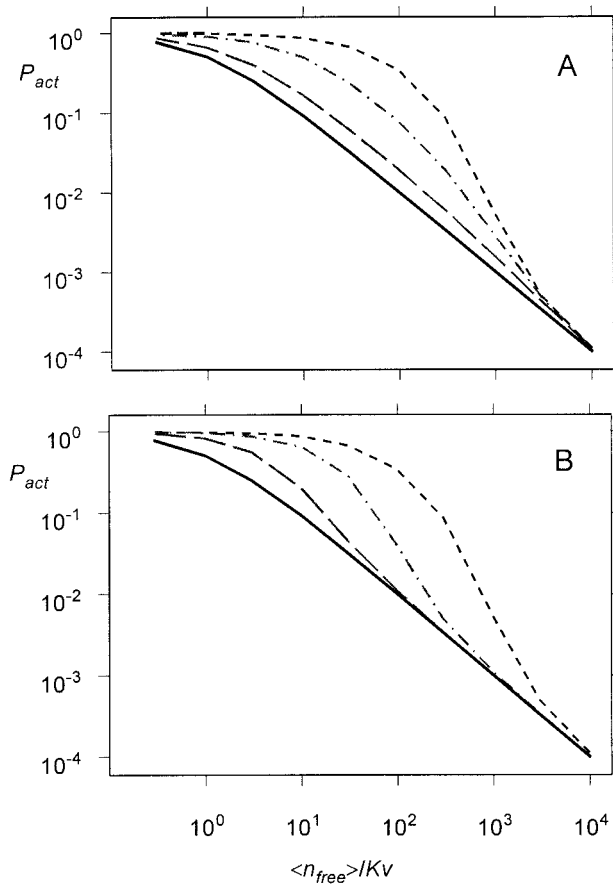


FIGURE 2 Gene activity with burst synthesis of repressor (or corepressor), $\beta = 100$, for all curves. The solid curve in both panels is the hyperbolic result from macroscopic theory. Broken curves are the results from the mesoscopic scheme (Eq. B2). On the x axis are the normalized numbers of free repressors $\langle n_{\text{free}} \rangle / Kv = \beta(k_s/k_d)/Kv$. (A) $Kv = 0.1$ for all curves; —, $k'_a/k_d = 0.01$; - - -, $k'_a/k_d = 0.1$; ·····, $k'_a/k_d \geq 10$. (B) $k'_a/k_d \gg 1$ for all curves; —, $Kv/\beta = 0.1$; - - -, $Kv/\beta = 0.01$; ·····, $Kv/\beta = 0.001$. When these results are due to corepressor fluctuations, the dissociation constant should be replaced by $Kv \rightarrow KvK_C/N$, and on the x axis would be the normalized number of free corepressors $\langle C_{\text{free}} \rangle N / KvK_C = \beta(k_s/k_d)N / KvK_C$.

2 A, solid curve). Fig. 2 B shows that SF disappears also when $\beta < Kv$, regardless of the rates of binding and dissociation. The reason is that in this region the average burst size is smaller than the dissociation constant, and therefore the fluctuations can only marginally influence the binding probability, so that the detailed balance constraint, Eq. 6, becomes important again. The macroscopic expectation is approached also when $\beta \ll 1$, i.e., in the limit of Poissonian fluctuations when Scheme 5 holds with detailed balance (data not shown).

Both cases discussed above approach the macroscopic sensitivity of control when the binding reactions (vertical steps) are much slower than the repressor number fluctuations (horizontal branches). In this limit Scheme 5, or its extensions, is approximately reduced to two independent

branches, and the system can “sense” only the average number of active repressors present. Then detailed balance holds, and the conditional average $\langle n \rangle_f$ can be calculated from the lower branch alone. When the fluctuations are determined by a linear process, like that depicted in Scheme 5 or like the burst process described in the Appendix, then $\langle n \rangle_f$ is also a linear function of the primary signal and SF vanishes. The more interesting limit is when the number fluctuations are much slower than the binding reactions, in which case noise can have a significant impact on both average activity and sensitivity. From these simplified schemes that have served to illustrate how detailed balance affects SF when signal molecules can both bind and dissociate from their targets, we now turn to more realistic situations.

In most cases, it is not the total number of repressors in a cell that controls gene expression, but the fraction of repressors that can bind strongly to DNA and thereby prevent initiation of transcription. The size of this fraction is controlled by inducers or corepressors that bind to the repressors, and the primary signal can in this important case be taken as the ratio of the rate constants of synthesis and degradation of these signaling ligands. This leads to a more complicated situation, but in important limits it can be described by a formalism similar to the one used for the simpler models described above.

Consider first the case where corepressors can bind only to repressor-operator complexes. Assume that there is a total of N repressors and C corepressors in the system and that the number of corepressors fluctuates slowly in comparison with all binding steps. Then a simple two-step binding reaction can be used to calculate the probabilities for the three different states of the operator: free (O_f), repressor bound (O_R), and repressor-corepressor bound (O_{RC}), conditional on there being C corepressors present:



The dissociation constant for corepressor is $K_C = k_{\text{diss}}^C/k'_a$. From Scheme 7 it is straightforward to calculate the probability that the operator is free and the gene is active:

$$P_{\text{act}}(C) = \frac{KvK_C/N}{C + K_C(1 + Kv/N)} \quad (8)$$

Since corepressor fluctuations are assumed to be much slower than all binding reactions, the processes that determine C will only sense the average number of free corepressors, $C - P_{\text{act}}(C)$, that are available for degradation or deactivation. By accounting for the bound corepressors, the distribution, P_C , over C can be calculated (Appendix), and the expected activity can be determined as the average,

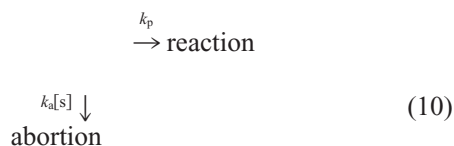
$$P_{\text{act}} = \sum_C P_C P_{\text{act}}(C) \quad (9)$$

Corepressors are usually present in much larger numbers than repressors. However, depending on how they are synthesized and degraded, they may display very large relative fluctuations. These, in turn, will generate fluctuations in the number of active repressors. If the repressor-operator binding (without corepressor) is so weak that $Kv \ll N$, the result is effectively the same as though corepressors by themselves repress gene activity with a dissociation constant KvK_c/N (Fig. 2 B). In this limit, the fluctuations make the repression curves much sharper than found macroscopically, i.e., there is SF. The case where only those repressors that are in complex with corepressor can bind the operator is more complicated, but calculations (not shown) give the same results in the appropriate limits. We have also analyzed the case where the repressor is under inducer control and found little difference from the macroscopic induction curve (data not shown), meaning that inducer fluctuations, in contrast to corepressor fluctuations, appear not to lead to SF.

The impact of SF in repressor-controlled systems depends critically on the time scales of the involved chemical reactions. A bacterial cell like *Escherichia coli* has a volume v corresponding roughly to 10^9 M^{-1} ; i.e., one molecule per cell corresponds to the concentration 10^{-9} M . Thus the requirement that $Kv < \beta$ (see Fig. 2) will easily be satisfied for dissociation constants $K < 10^{-9} \text{ M}$; e.g., the *lac* repressor-operator dissociation constant corresponds to $Kv = 0.001\text{--}0.01$. The maximum diffusion-limited association rate constants are of the order 10^8 to $10^9 \text{ M}^{-1}\text{s}^{-1}$, so that k'_a is at most of the order $0.1\text{--}1 \text{ s}^{-1}$. For maximum SF, the number fluctuations in repressor or corepressor should be slower than this.

STOCHASTIC FOCUSING, FLUCTUATIONS, AND SENSITIVITY

Previously (Paulsson et al., 2000) we considered the ubiquitous hyperbolic inhibition mechanism as arising from a branching reaction like



For this scheme, the reaction rate is proportional to a parameter q that depends on the concentration $[s]$ of a signal molecule as

$$q = \frac{1}{1 + [s]/K} \quad (11)$$

where $K = k_p/k_a$. Thus, if the probability that there are n molecules at the time of the branching reaction in Eq. 10 is p_n , and n does not change significantly during the time window of an individual branching reaction, the effective

reaction probability q in Eq. 11 must be calculated as an average $\langle q \rangle$, where

$$\langle q \rangle = \sum_{n=0}^{\infty} p_n q(n) = \sum_{n=0}^{\infty} p_n \frac{1}{1 + n/Kv} \quad (12)$$

It was shown by Paulsson et al. (2000) that signal noise arising naturally from biochemical reactions can increase the sensitivity, measured by amplification factors, of such kinetic control mechanisms. This noise-generated increase of sensitivity amplification was termed stochastic focusing (SF) and was exemplified by hyperbolic inhibition in combination with a number of signal noise distributions, including the Poissonian and negative binomial (NB). It was shown how the fluctuations could be exploited to transcend macroscopically defined sensitivity limits because the average of $1/(1 + n/Kv)$ calculated in Eq. 12 generally differs from that given by the average concentration in Eq. 11, $1/(1 + [s]/K)$.

However, for repressor-operator binding, Eq. 12 cannot be adopted as the stochastic counterpart of Eq. 2, without a careful analysis of the probabilities p_n . The reason for this is that the probability that the operator is free at any moment does not depend on a single binding event, as in Scheme 2, but on many previous association and dissociation events. Therefore the probability that the system contains a certain total number of repressors will depend on whether the operator is free or occupied, so that Eq. 12 must be replaced by an expression that takes this more complex reality into account. By including all association and dissociation events of repressors in the complete reaction scheme (Scheme 5), it becomes clear that SF is an out-of-equilibrium effect that disappears whenever the stationary distributions are constrained by detailed balance, as in equilibrium schemes.

In the perspective of Eq. 4, it is nonlinearities in the conditional average $\langle n \rangle_f$ that are required for SF to appear. The same phenomenon can also be understood from the perspective of Eq. 12. Here, SF arises or not, depending on the shape of the probability distribution p_n for the total number of (active) repressors in the system in relation to the probability $q(n) = 1/(1 + n/Kv)$ that a promoter is free, given n (active) repressors. The crux of the matter is that in the repressor case the signal number probabilities p_n cannot be calculated without taking into account the influence of the regulated process, i.e., operator binding, on these very probabilities. If, to illustrate the point, a repressor has just dissociated from the operator, then there is at least one free repressor in the cytoplasm. This means that the probability of zero free repressors, given that the operator was just cleared, is radically lower than is calculated for processes in which the probability distribution of signal molecule numbers is independent of events in the regulated process. If, in contrast, also bound signal molecules can be irreversibly

removed from the system without entering the free state then the probability distribution p_n can be obtained exactly or as a good approximation without taking the regulated process into account. In this case SF is operative also when signal fluctuations are Poissonian or binomial (Paulsson et al., 2000).

Repressor binding is an important and simple example of a control circuit that can exploit SF for increased sensitivity, provided that the fundamental detailed balance constraint is violated. As seen, such violations may occur when signal fluctuations are coherent in the sense that they involve more than a single particle or when repressors are irreversibly removed from the bound state at the expense of free energy. Most commonly, repressors are regulated by smaller molecules, like corepressors, that bind to and activate them for binding to DNA. Coherent number fluctuations of these small regulatory molecules, e.g., through synthesis and degradation or consumption in downstream metabolic pathways, can also lead to SF. Such reactions are dissipative and therefore are often associated with coherent fluctuations opening the evolutionary path to SF. Another system option is that corepressors with the aid of free energy can be brought to their free state faster than otherwise allowed by the detailed balance constraint. This is analogous to the case where repressor molecules are irreversibly removed directly from their bound state, and it allows for SF also when signal molecules display single particle fluctuations.

Detailed balance can be broken in yet another way for systems where repressors are not degraded. Consider again a cell population where expression from an operon is controlled by repressor (e.g., *lac* repressor) binding to a single operator site. In the simplest case repressor molecules are not degraded but constantly diluted through cell growth. At each cell division, the repressor molecules will be partitioned according to a deformed binomial distribution: free repressors will be distributed randomly (binomially), while a repressor bound to a chromosome will tend to follow this to a daughter cell. This situation was studied theoretically by Berg (1978), and it was found that the resulting statistical distribution of repressors over different cells can be very broad. Based on this distribution, it is straightforward (Appendix) to calculate the expectation value for the activity of the controlled gene as a function of the expected number of repressors per cell, and a very strong SF effect is predicted (Fig. 3, *dashed curves*). In this case, detailed balance is broken in two ways: by the assumed burst production of repressors and by the partitioning at cell division where the concentrations of repressors in a cell can change abruptly. In this system, the control in individual cells is erratic because of the longevity (cell generation time) of repressor fluctuations, but the total enzyme activity in the population is predicted to respond very sharply to changes in the average repressor concentration (Fig. 3). Below the “knee” of the curves in Fig. 3, the activity is determined primarily by the average repressor concentration, as in Eq. 11, and the slope

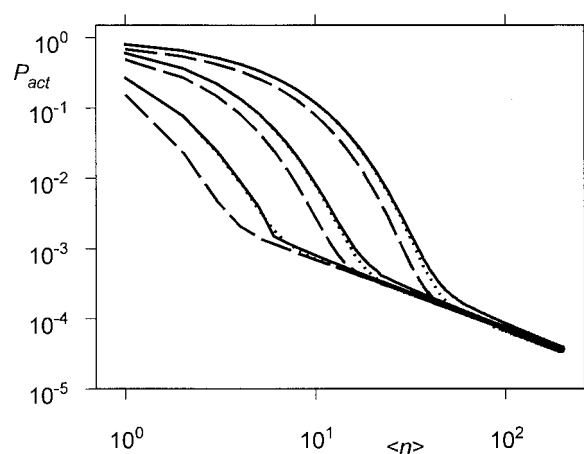


FIGURE 3 Population average of gene activity when repressors are not degraded but diluted through random partitioning at cell division. $K_V = 0.01$. On the x axis is the average number of repressors produced per cell cycle, $\langle n \rangle$; the average number per cell in the population is $\langle n \rangle / \ln 2$. —, Strict binomial partitioning without accounting for operator-bound repressors. ····, The same, using the approximation in Eq. A12. — —, Binomial partitioning only of repressors that are not operator bound, using Eq. A12. The upper set of curves is with burst size $\beta = 20$, the middle set with $\beta = 5$, and the lowest set with $\beta = 0.1$.

is -1 . Above the “knee,” cells with no repressors in them dominate the average activity, and the slope is considerably steeper (SF).

CONCLUDING REMARKS

Regulatory reaction rates in living cells generally depend nonlinearly on randomly fluctuating concentrations. This means that noise can be exploited for anything from non-genetic individuality (Spudich and Koshland, 1976; Berg, 1978) to sensitivity amplification (Paulsson et al., 2000), robustness, or even predictability (Paulsson and Ehrenberg, 2000). As shown in the present analysis, repressor-operator binding, which is perhaps the most important intracellular control motif, can exploit random fluctuations in repressor or corepressor concentration for sharper regulation. This requires that detailed balance is broken, and this fundamental physical constraint determines general design principles for control mechanisms of repressor type that use SF to amplify sensitivity. One such principle is to generate coherent fluctuations in signal molecule numbers, which can be implemented by burst synthesis or degradation, as well as by many other kinetic schemes (Paulsson et al., 2000). Another is irreversible removal of signal molecules from the bound state at a free energy cost.

Fluctuations can enhance the sensitivity of regulated processes that from a macroscopic viewpoint (i.e., neglecting fluctuations) are expected to be gradual, like the hyperbolic ones considered here and by Paulsson et al. (2000). In contrast, for a process that is expected to be very sharp, like

the zero-order ultrasensitivity mechanism (Goldbeter and Koshland, 1981), fluctuations in the signal molecules will in general blur the response and make it much more gradual (Berg et al., 2000). In genetic control, like repressor control, signal fluctuations can have both focusing and defocusing effects, making the response sharper or more blurred, depending on the precise molecular mechanisms involved. However, in the examples considered above, fluctuations do not defocus the control, i.e., make it less sensitive than the hyperbolic. It should also be noted that even in cases where sensitivity is increased only marginally (the slope is increased at most by a factor of 2 in Fig. 2), the predicted activity in the presence of fluctuations can be much larger than expected from the hyperbolic binding curve with the same parameter values. This is because fluctuations can have a significant impact on expectation values in nonlinear schemes.

The main point of this paper, that fluctuation-enhanced sensitivity (SF) in biological control systems must operate out of equilibrium in such a way that detailed-balance constraints are removed, is reminiscent of a similar requirement in the case of enhanced enzymatic selectivity through kinetic proofreading (Hopfield, 1974; Ninio, 1975). Moreover, this mechanism, where a small structural difference between a cognate and noncognate substrate can be probed several times by an enzyme to obtain virtually infinite accuracy, strictly depends on the extent to which detailed balance is broken (Ehrenberg and Blomberg, 1980). Breaking detailed balance in proofreading reactions is in general associated with excess hydrolysis of nucleoside triphosphates, and this was used to verify the existence of proofreading of amino acids in the aminoacylation reaction (Hopfield et al., 1976) and of tRNAs by ribosomes in bacterial protein synthesis (Thompson and Stone, 1977; Ruusala et al., 1982). Proofreading of substrate molecules is an intrinsic property of certain biosynthetic enzymes and can therefore be studied by biochemical experiments in the test tube. Stochastic focusing, in contrast, is a system property and depends on the statistical distribution of signal molecules in intact cells.

In general, this makes experimental verification of the mechanism much more challenging, because it requires detailed characterization of control systems in situ and, in particular, knowledge of signal molecule distributions in single cells. The necessary experimental tools for single-cell analysis are developing rapidly, and we are therefore optimistic that such experiments will become feasible in the near future. For a more immediate verification of SF in repressor control of gene expression we will propose a slightly less ambitious experimental design. It is based on the fact that although SF depends on the random nature of reactions in individual cells and disappears if all cell contents are mixed, stochastic focusing can be clearly seen in averages taken over large populations of single cells. Therefore SF can be demonstrated experimentally by studying the

total activity of a particular repressor-controlled gene in a large population of cells where the average repressor concentration is changed. If, furthermore, the control system is sufficiently simple and the distribution of signal molecules in single cells can be calculated with reasonable confidence, verification of SF can be carried out in a simple way. The theoretical results in Fig. 3 describe such a case and display very sensitive responses in gene expression when the average repressor concentration is varied. These results relate to a simple experimental system where repressors are constitutively expressed and where they are not degraded by proteolytic activities. The results apply in particular to a situation where the average level of *lac* repressors, produced in bursts by repeated translations of single messengers, is varied and the resulting population-averaged activity of the *lac* operon is measured. The average number of repressor molecules (e.g., controlled by changing the strength of the promoter for the repressor gene by sequence variations) can be directly measured with standard methods. The expression from the *lac* operon can conveniently be obtained from the β galactosidase activity per cell mass. SF is revealed in a plot of the logarithm of β galactosidase activity versus the logarithm of the repressor concentration by slopes with negative values significantly larger than 1 (see Fig. 3).

To make precise predictions of repressor molecule distributions and for large SF effects it is important that the repressor gene is expressed constitutively; in particular, it is important that it is not under negative feedback control by its own gene product. This has been conventional wisdom for the *lac* repressor gene, but may require careful consideration. The simple analysis suggested here also requires that there is only one important binding site for the *lac* repressor, which is not the case for the wild-type *lac* operon. For the variations shown in Fig. 3, SF effects in the proposed experiment will be most pronounced when repressor concentrations are reduced below wild type (~ 10 – 20 molecules per cell) rather than increased, as in well-known 10- or 100-fold overproducing *E. coli* strains (e.g., Müller-Hill, 1971). New genetic constructs may therefore be needed for the suggested approach.

APPENDIX: BREAKING DETAILED BALANCE

Degradation of DNA-bound repressor

Detailed balance in Scheme 5 is broken when operator-bound repressors are also degraded. If the rate constant of degradation is k_d for both free and bound repressors, Scheme 5 will be expanded by extra diagonal arrows from all states $(n + 1)_b$ to $(n)_f$ with rate k_d . Because synthesis and breakdown in this way are independent of binding, the overall distribution describing the number of repressor molecules in the system must be Poissonian:

$$p_n = \frac{\lambda^n}{n!} e^{-\lambda} \quad (\text{A1})$$

where $\lambda = k_s/k_d = \langle n \rangle$ is the average number. The degradation of the bound repressor serves as an extra dissociation step, so that the overall binding in the stationary state must now satisfy (cf. Eq. 3)

$$k'_a \sum_n n p_n^f = (k_{\text{diss}} + k_d) \sum_n p_n^b \quad (\text{A2})$$

In the same way as in Eq. 4, the probability that the operator is free is now

$$P_{\text{act}} = \frac{1}{1 + k'_a \langle n \rangle_f / (k_{\text{diss}} + k_d)} = \frac{1}{1 + \langle n \rangle_f / K'} \quad (\text{A3})$$

where $K' = (k_{\text{diss}} + k_d)/k'_a$ is an effective dissociation constant. Although the overall distribution is a simple Poissonian in this case, to calculate the sensitivity of the control one must find the conditional distribution p_n^f , or at least the average $\langle n \rangle_f$.

At the stationary state, the probabilities of the expanded Scheme 5 satisfy

$$0 = \frac{dp_n^f}{dt} = k_{\text{diss}} p_n^b + k_d p_{n+1}^b + k_s p_{n-1}^f + (n+1) k_d p_{n+1}^f - [k_s + n(k_d + k'_a)] p_n^f \quad (\text{A4})$$

Furthermore, from Eq. (A1),

$$p_n^b = \frac{\lambda^n}{n!} e^{-\lambda} - p_n^f \quad (\text{A5})$$

Inserting (A5) in (A4) and introducing $A = k'_a/k_d$ and $D = k_{\text{diss}}/k_d$, one finds

$$[\lambda + D + n(A+1)] p_n^f - n p_{n-1}^f - n p_{n+1}^f = \frac{\lambda^n}{n!} e^{-\lambda} \left(D + \frac{\lambda}{n+1} \right), \quad \text{for } n > 0 \quad (\text{A6a})$$

$$p_0^f = p_0 = e^{-\lambda} \quad (\text{A6b})$$

Introducing the generating function $F(z) = \sum_{n=0}^{\infty} z^n p_n^f$, multiplying each of the Eqs. A6 by z^n , and summing over all n gives

$$z[(A+1)z - 1]F'(z) + [1 + (D+\lambda)z - \lambda z^2]F(z) = (Dz + 1)e^{-\lambda(1-z)} \quad (\text{A7})$$

The generating function must satisfy

$$F(1) = \sum_{n=0}^{\infty} p_n^f = P_{\text{act}} \quad (\text{A8})$$

The general solution to Eq. A7 is

$$F(z) = \frac{e^{-\lambda(1-z/(A+1))} z}{g(z)((A+1)z - 1)} \left\{ \int_1^z \frac{(Dx + 1)e^{(\lambda A/(A+1))x} g(x)}{x^2} dx + C \right\} \quad (\text{A9a})$$

where

$$g(z) = \left(z - \frac{1}{A+1} \right)^{D(A+1) + \lambda A/(A+1)^2} \quad (\text{A9b})$$

This solution automatically satisfies the boundary condition $F(0) = p_0 = p_0^f = e^{-\lambda}$ at $z = 0$, irrespective of the value of the integration constant C . However, the factor in front of the curly brace in Eq. A9a diverges as $z \rightarrow 1/(A+1)$. Because $F(z)$ must be finite for $|z| \leq 1$, C must be chosen so that $\{\dots\} \rightarrow 0$ when $z \rightarrow 1/(A+1)$. This gives

$$P_{\text{act}} = F(1) = \frac{1}{Ag(1)} \int_{1/(A+1)}^1 \frac{1}{x^2} (Dx + 1) e^{-(\lambda A/(A+1))(1-x)} g(x) dx \quad (\text{A10})$$

where $A = k'_a/k_d$, $D = k_{\text{diss}}/k_d$, $\lambda = k_s/k_d$, with $g(x)$ from Eq. A9b. The results for some parameter values are shown in Fig. 1. The numerical integrations described here and below were carried out using Mathcad (Mathsoft) software.

In the limit where the association-dissociation steps are much faster than degradation, $A, D \rightarrow \infty$, while $k_{\text{diss}}/k'_a = D/A = Kv$, Eq. A10 reduces to

$$P_{\text{act}} = Kv \int_0^1 x^{Kv-1} e^{-\lambda(1-x)} dx \quad (\text{A11})$$

Equation A11 is an integral representation of the sum in Eq. 12 when p_n is Poissonian, so that in this limit SF for repressors works exactly as shown previously for the branching type reaction (Paulsson et al., 2000) (Fig. 1, *dashed line*).

Equation A11 is, in fact, the integral representation for Eq. 12 also when p_n is not Poissonian, provided that $e^{-\lambda(1-x)}$ is replaced with the appropriate generating function for the actual distribution p_n . Equation 12 gives the expected activity also in cells where repressors are not degraded but only diluted through partitioning at cell division (Berg, 1978). In this case, P_{act} depends explicitly on the time t in the cell cycle through a time-dependent repressor distribution, $p_n(t)$, and cell volume, $v(t)$. In Eq. A11 we use the time-dependent generating function given in equation 34 of Berg (1978). This generating function, based on burst synthesis and a totally random partitioning of repressors at cell division, was adapted for random repressor mRNA production. Thus, the population average of the activity (Fig. 3, *solid curves*) was calculated by taking the appropriate time average followed by numerical integration of Eq. A11. When operator binding is strong, $Kv \ll 1$, Eq. 12 can be approximated by separating out the cells with no repressors (average probability p_0) and full activity and considering the activity in the rest of the cells as determined by the average repressor numbers:

$$P_{\text{act}} \approx p_0 + \frac{Kv(1-p_0)}{Kv + \langle n \rangle / \ln(2)} \quad (\text{A12})$$

Here v is the population average of the cell volume, $\langle n \rangle$ is the average number of repressors produced during a cell cycle, and $\langle n \rangle / \ln(2)$ is the population average per cell. The results from this approximation are nearly indistinguishable from the proper averaging of Eq. 12 (cf. the *solid* and *dotted curves* in Fig. 3). The full repressor distribution has not been derived for the more realistic case of repressor partitioning, where only free repressors are distributed randomly (binomially) while a repressor bound to the operator site on a chromosome follows it to a daughter cell, but p_0 and $\langle n \rangle$ are known (Berg, 1978). To describe this case we therefore used Eq. A12 to generate the dashed curves in Fig. 3. The approximation (Eq. A12) was also tested and holds well (data not shown) for the case of Poissonian repressor production (i.e., random production without bursts) by repeated numerical iteration of repressor partitioning at cell division.

Burst synthesis of repressor

The probability, h_r , that r repressor molecules are synthesized from one mRNA with an exponentially distributed lifetime is geometrically distributed (Berg, 1978):

$$h_r = \frac{1}{1 + \beta} \left(\frac{\beta}{1 + \beta} \right)^r \quad (\text{B1})$$

β is the average number of molecules produced per mRNA. The mRNA is synthesized with rate k_s , and free repressors are degraded by the first-order rate constant k_d . Scheme 5, expanded with the burst synthesis steps, leads to the master equations,

$$\begin{aligned} \frac{dp_n^f}{dt} = & k_d(n+1)p_{n+1}^f - k_d n p_n^f + k_s \sum_{r=1}^n h_r p_{n-r}^f \\ & - k_s \frac{\beta}{1 + \beta} p_n^f + k_{\text{diss}} p_n^b - k'_a n p_n^f \end{aligned} \quad (\text{B2})$$

$$\frac{dp_n^b}{dt} = k_d n p_{n+1}^b - k_d(n-1)p_n^b + k_s \sum_{r=1}^n h_r p_{n-r}^b$$

$$- k_s \frac{\beta}{1 + \beta} p_n^b - k_{\text{diss}} p_n^b + k'_a n p_n^f$$

Introducing the generating functions, $F(z) = \sum_{n=0}^{\infty} z^n p_n^f$ and $G(z) = \sum_{n=1}^{\infty} z^{n-1} p_n^b$, in analogy with Eq. A7 above, gives, at the stationary state,

$$\begin{aligned} 0 = & (1-z)F'(z) - \frac{\lambda\beta(1-z)}{1 + \beta(1-z)} F(z) + DzG(z) - AzF'(z) \\ 0 = & (1-z)G'(z) - \frac{\lambda\beta(1-z)}{1 + \beta(1-z)} G(z) - DG(z) + AF'(z) \end{aligned} \quad (\text{B3})$$

$A = k'_a/k_d$, $D = k_{\text{diss}}/k_d$, and $\lambda = k_s/k_d$, as before. When there are no binding reactions ($A = D = 0$) the solution is the generating function for the negative binomial distribution (NB) with average $\beta\lambda$ and variance $\beta(\beta + 1)\lambda$:

$$F(z) + G(z) = [1 + \beta(1-z)]^{-\lambda} \quad (\text{B4})$$

The requirement that all probabilities sum to 1 leads to the boundary condition (at $z = 1$)

$$F(1) + G(1) = 1 \quad (\text{B5})$$

The average number of free repressors in the system is

$$\langle n_{\text{free}} \rangle = \sum_n [n p_n^f + (n-1)p_n^b] = F'(1) + G'(1) = \beta\lambda \quad (\text{B6})$$

The probability

$$P_{\text{act}} = \sum_n p_n^f = F(1) \quad (\text{B7})$$

that no repressor is bound can be found by numerical integration of the differential equations (Eq. B3), although the boundary condition, Eq. B7, is the primary quantity to be determined. This is done by choosing that value of $F(1)$ that produces solutions $F(z)$ and $G(z)$ that are continuous

functions at $z = 1/(A + 1)$ (i.e., the same potential divergence point as for Eq. A9) and satisfy $0 \leq F(z) \leq 1$ and $0 \leq G(z) \leq 1$ for $0 \leq z \leq 1$. For most parameter values, these conditions are sufficient to provide a value for $P_{\text{act}} = F(1)$ that is well defined. The results for some parameter values are shown in Fig. 2 A.

Corepressor fluctuations

Consider the situation described by Scheme 9 that is valid for corepressor activation at a given number of corepressors, C . Because fluctuations in this number were assumed to be much slower than all binding processes, the synthesis-degradation of corepressors will sense only the average number of free corepressors given by

$$\langle C_{\text{free}}(C) \rangle = C - \frac{KvK_C/N}{C + K_C(1 + Kv/N)} \quad (\text{C1})$$

where the last term accounts for corepressors bound at a repressor-operator complex (Eq. 8). Thus for any given C , only $\langle C_{\text{free}}(C) \rangle$ corepressors are unbound by repressor and are accessible for degradation or usage in metabolism. Assuming that corepressors are produced in a burst process like the one described in the previous section, with parameters $\lambda = k_s/k_d$ and β , the master equation describing changes in the probability, P_C , of having C corepressors at the stationary state is given by

$$\begin{aligned} 0 = & (C+1 - \langle C_{\text{free}}(C+1) \rangle) P_{C+1} - (C - \langle C_{\text{free}}(C) \rangle) P_C \\ & + \lambda \sum_{r=1}^C h_r P_{C-r} - \frac{\lambda\beta}{1 + \beta} P_C \end{aligned} \quad (\text{C2})$$

in analogy with Eq. B2. Using Eq. C1 and introducing the generating function $Q(z) = \sum_C z^C P_C$, Eq. C2 can be transformed to

$$\begin{aligned} zQ' - Q + Bz^{-B-K_C} \int_0^z x^{B+K_C-1} Q(x) dx - \frac{\lambda\beta z}{1 + \beta(1-z)} Q \\ = 0 \end{aligned} \quad (\text{C3})$$

where $B = K_C Kv/N$. Introducing the new function

$$f(z) = Bz^{-B-K_C} \int_0^z x^{B-1} Q(x) dx \quad (\text{C4})$$

Eq. C3 can be transformed to a second-order differential equation for f that can be integrated numerically with the boundary conditions

$$f(1) = P_{\text{act}} \quad (\text{C5})$$

$$f'(1) = B - (B + K_C) P_{\text{act}} \quad (\text{C6})$$

The probability that the operator is free and the gene is active, P_{act} , is given by the sum in Eq. 9. The boundary condition (Eq. C5) comes from the fact that $f(1)$ in Eq. C4 is the integral representation of this sum. By choosing P_{act} so that $0 \leq Q(z) \leq 1$ holds for all values of z within $0 \leq z \leq 1$, a solution can be found for any values of the parameters λ , β , K_C , and $B = K_C Kv/N$. When repressor action is controlled by corepressor concentration, repressor-operator binding must be weak when corepressor is not bound, i.e., $Kv \gg N$. In this limit, $B \gg K_C$ and the results are identical to those shown in Fig. 2 B.

We thank Johan Andersson for valuable comments on the manuscript.

This work was supported by the National Graduate School of Scientific Computing, the Swedish Natural Science Research Council, and the Swedish Research Council for Engineering Sciences.

REFERENCES

- Arkin, A., J. Ross, and H. H. McAdams. 1998. Stochastic genetic analysis of developmental pathway bifurcation in phage lambda-infected *Escherichia coli* cells. *Genetics*. 149:1633–1648.
- Berg, O. G. 1978. A model for the statistical fluctuations of protein numbers in a microbial population. *J. Theor. Biol.* 71:587–603.
- Berg, O. G. 1983. Time-averaged chemical potential of proteins and the detailed-balance principle. (An alternative viewpoint). *Proc. Natl. Acad. Sci. USA*. 80:5302–5303.
- Berg, O. G., and C. Blomberg. 1977. Mass action relations in vivo with application to the *lac* operon. *J. Theor. Biol.* 67:523–533.
- Berg, O. G., J. Paulsson, and M. Ehrenberg. 2000. Fluctuations and quality of control in biological cells: zero-order ultrasensitivity reinvestigated. *Biophys. J.* 79:1228–1236.
- Cook, D. L., A. N. Gerber, and S. J. Tapscott. 1998. Modelling stochastic gene expression: implications for haploinsufficiency. *Proc. Natl. Acad. Sci. USA*. 95:15641–15646.
- Ehrenberg, M., and C. Blomberg. 1980. Thermodynamic constraints on kinetic proofreading in biosynthetic pathways. *Biophys. J.* 31:333–358.
- Eisenberg, D., and D. Crothers. 1979. *Physical Chemistry with Applications to the Life Sciences*. Benjamin/Cummings, Menlo Park, CA.
- Goldbeter, A., and D. E. Koshland, Jr. 1981. An amplified sensitivity arising from covalent modification in biological systems. *Proc. Natl. Acad. Sci. USA*. 78:6840–6844.
- Guptasarma, P. 1995. Does replication-induced transcription regulate synthesis of the myriad low copy number proteins of *Escherichia coli*? *Bioessays*. 17:987–997.
- Hopfield, J. J. 1974. Kinetic proofreading: a new mechanism for reducing errors in biosynthetic processes requiring high accuracy. *Proc. Natl. Acad. Sci. USA*. 71:4135–4139.
- Hopfield, J. J., T. Yamane, V. Yue, and S. M. Coutts. 1976. Direct experimental evidence for kinetic proofreading in amino acylation of tRNA^{lle}. *Proc. Natl. Acad. Sci. USA*. 73:1164–1168.
- Ko, M. S. H. 1992. Induction mechanism of a single gene molecule: stochastic or deterministic? *Bioessays*. 14:341–346.
- McAdams, H. H., and A. Arkin. 1997. Stochastic mechanism in gene expression. *Proc. Natl. Acad. Sci. USA*. 94:814–819.
- McAdams, H. H., and A. Arkin. 1999. It's a noisy business! Genetic regulation at the nanomolar scale. *Trends Genet.* 15:65–69.
- Müller-Hill, B. 1971. Lac repressor. *Angew. Chem. Int. Ed. Engl.* 10:160–172.
- Ninio, J. 1975. Kinetic amplification of enzyme discrimination. *Biochimie*. 57:587–595.
- Paulsson, J., O. G. Berg, and M. Ehrenberg. 2000. Stochastic focusing: fluctuation-enhanced sensitivity of intracellular regulation. *Proc. Natl. Acad. Sci. USA*. 97:7148–7153.
- Paulsson, J., and M. Ehrenberg. 1998. Trade-off between segregational stability and metabolic burden: a mathematical model of plasmid ColE1 replication control. *J. Mol. Biol.* 279:73–88.
- Paulsson, J., and M. Ehrenberg. 2000. Random signal fluctuations can reduce random fluctuations in regulated components of chemical regulatory networks. *Phys. Rev. Lett.* 84:5447–5450.
- Rényi, A. 1953. Treating chemical reactions using the theory of stochastic processes. *MTA Alk. Mat. Int. Közl.* 2:83–101 (in Hungarian).
- Ruusala, T., M. Ehrenberg, and C. G. Kurland. 1982. Is there proofreading during polypeptide synthesis? *EMBO J.* 1:741–745.
- Savageau, M. A. 1976. *Biochemical Systems Analysis: A Study of Function and Design in Molecular Biology*. Addison-Wesley, Reading, MA.
- Spudich, J. L., and D. E. Koshland, Jr. 1976. Non-genetic individuality: chance in the single cell. *Nature*. 262:467–471.
- Thompson, R. C., and P. J. Stone. 1977. Proofreading of the codon-anticodon interaction on ribosomes. *Proc. Natl. Acad. Sci. USA*. 74:198–202.